การจำแนกรูปแบบการเกิดดีสชาร์จบางส่วนในอุปกรณ์ไฟฟ้าแรงสูง โดยวิธีเพอร์เซ็ปตรอนหลายชั้น

Classification of Pattern Partial Discharge (PD) in High Voltage Equipment by Multilayer Perceptron Method

อานันทวัฒน์ คุณากร สาวิณี หลุดพา* และ พีรวุฒิ ยุทธโกวิท

Anantawat Kunakorn, Savinee Ludpa* and Peerawut Yutthagowith

Received: 9 December 2021, Revised: 26 May 2022, Accepted: 8 June 2022

บทคัดย่อ

งานวิจัยนี้นำเสนอการจำแนกทางสถิติและการประยุกต์ใช้โครงข่ายประสาทเทียมโดยใช้เพอร์เซ็ปตรอนหลายชั้น เพื่อจำแนกรูปแบบการเกิดดิสชาร์จบางส่วน (PD) ออกเป็น 4 ประเภท คือ โคโรนาดิสชาร์จทางด้านแรงสูงโคโรนาดีสชาร์จทางด้านแรงต่ำดีสชาร์จภายใน และดีสชาร์จตามผิว การวิเคราะห์รูปแบบโดยมีตัวแปรอิสระ 9 ตัวแปรจะพิจารณาจากการกระจายความสัมพันธ์ระหว่าง Phi - q - n ของข้อมูลการเกิดดิสชาร์จบางส่วนแต่ละประเภท ซึ่งประกอบด้วยค่าการคำนวณคุณลักษณะด้วยวิธีสถิติ ซึ่งคำนวณจากการกระจายขนาดของดิสชาร์จบางส่วนเฉลี่ยตามมุมเฟสของแรงดัน ($H_{qn}(\phi)$) และการกระจายจำนวนครั้งที่เกิดดิสชาร์จบางส่วนซ้ำตามมุมเฟสแรงดัน ($H_n(\phi)$) โดยคำนวณจากการกระจายความสัมพันธ์ระหว่างขนาดของดิสชาร์จบางส่วน (q), มุมเฟสของแรงดันทดสอบ (ϕ) และจำนวนครั้งที่เกิดดิสชาร์จบางส่วนซ้ำ (n) จะได้ค่าความเบ้เอียงของการกระจายข้อมูลเทียบกับการกระจายปกติ, ความแหลมคมของการกระจายข้อมูลเทียบกับการกระจายปกติมีทั้งค่าบวกและค่าลบ ซึ่งจะได้ตัวแปรอิสระ 9 ตัวแปรแล้วจึงนำตัวแปรอิสระทั้ง 9 ตัวแปร มาใช้ในการจำลองโครงข่ายประสาทเทียมสำหรับจำแนกรูปแบบการเกิดดิสชาร์จบางส่วนได้ โดยแบ่งข้อมูลออกเป็น 2 กลุ่มสำหรับข้อมูลในการเรียนรู้และข้อมูลสำหรับการทดสอบ ข้อมูลสำหรับการเรียนรู้และการทดสอบแบบจำลองสถาปัตยกรรมของโครงข่ายประสาทเทียมในบทความนี้ คัดเลือกให้มีความซับซ้อนน้อยที่สุด โดยใช้เพอร์เซ็ปตรอนหลายชั้น ซึ่งผลการวิจัยพบว่าแบบจำลองโครงข่ายประสาทเทียมประกอบด้วย 1 ชั้นซ่อนเท่านั้น และผลลัพธ์ที่ได้มีประสิทธิภาพในการจำแนกรูปแบบการเกิดดิสชาร์จบางส่วน โดยมีความแม่นยำในการจำแนก 100% ซึ่งสามารถนำแบบจำลองดังกล่าวจำแนกรูปแบบการเกิดดิสชาร์จบางส่วนและสามารถนำไปพัฒนาจำแนกการเกิดดิสชาร์จบางส่วนของอุปกรณ์ไฟฟ้าแรงสูงได้

คำสำคัญ: เพอร์เซ็ปตรอนหลายชั้น, ดิสชาร์จบางส่วน, การจำแนก, อุปกรณ์ไฟฟ้าแรงสูง, โคโรนาดิสชาร์จ

สาขาวิศวกรรมไฟฟ้า คณะวิศวกรรมศาสตร์ สถาบันเทคโนโลยีพระจอมเกล้าเจ้าคุณทหารลาดกระบัง เขตลาดกระบัง กรุงเทพมหานคร 10520

Department of Electrical Engineering, School of Engineering, King Mongkut's Institute of Technology Ladkrabang, Ladkrabang, Bangkok 10520, Thailand.

*Corresponding author, e-mail: l.savinee@gmail.com

ABSTRACT

This paper proposes a statistical classification based on an application of neural networks by Multilayer Perceptron (MLP) to classify Partial Discharge (PD) patterns into four categories in corona: high voltage side in air, corona at low voltage side in air, internal discharge and surface in air. There are 9 independent variables from fingerprint analysis which mainly are skewness, kurtosis, asymmetry and cross correlation following Phi - q - n PD patterns. PD patterns were used for classification which consists of statistical attribute calculation values. This is calculated from the $H_{qn}(\phi)$ distribution (average PD size distribution based on the voltage phase angle) and $H_n(\phi)$ distribution (the number of PD repeat distributions based on the voltage phase angle) distribution calculated from the $H_{qn}(\phi)$ distribution. (It was calculated from the relationship distribution between the magnitude of the PD(q) , the phase angle of the test voltage (ϕ) , and the number of PD repetitions (n)). All 9 variables were then used in the neural network simulation for partial discharge pattern identification. The approach for constructing the network divides the data into two groups for training data and testing data. The forms for training the model and the pattern for testing the model. The architecture of artificial neural networks in this paper is selected to below complexity as possible using multiple layers of perceptron. The results show that only a hidden layer in the model has a good performance to classify PD pattern with the classification accuracy of 100%. The proposed method can be used to analyze and classify partial discharge patterns and it can be developed to test the partial discharge of high voltage equipment.

Key words: multilayer perceptron (MLP), partial discharge (PD), classification, high voltage equipment, corona discharge

INTRODUCTION

The occurrence of a fault (fault) in the power system. One of the main causes is insulation failure in high-voltage transmission systems. Partial Discharge (PD) is the main factor causing insulation failure. Therefore, the IEC 60270 Standard (IEC, 2000) requires that PD be measured or detected before the device is put into service. Insulating properties test engineers need to study and classify PD characteristics in order to determine which type of PD occurs, such as corona discharge, surface discharge or internal discharge, etc. Such information is important to manufacturers of high voltage equipment. In the past, high voltage laboratories and users of high voltage equipment learned and recognized PD patterns by visually observing the oval signals on an oscilloscope screen and interpreting them based on the tester's experience. Nowadays, computers are used to analyze PD by programmable simulation. It can recognize the pattern of PD formation, making it easy for the tester to analyze, classify and tell the cause of faults occurring in the insulation system. There are more diverse methods and various pattern recognition methods that have been proposed, such as expert systems (Gopal *et al*., 2004), statistical analysis (Chatpattananan, 2006; Chatpattananan *et al*., 2006a; Chatpattananan *et al*., 2006b; Pattanadech and Nimsanong, 2014), fuzzy clustering (Gopal *et al*., 2004; Tomsovic *et al*., 1993), neural networks (Cho and Oh, 1997; Gulski and Krivda, 1993; Pattanadech *et al*., 2015a; Zhang *et al*., 2005), KMeans (Chatpattananan *et al*., 2006c), Regression Estimation (Ludpa *et al*., 2008; Pattanadech *et al*., 2015b), Expert systems and fuzzy approaches require human expertise. However, there are some problems with the acquisition and maintenance of databases. Neural networks can gain direct experience from the training data and overcome some of the shortcomings of the expert system. Therefore, this paper proposes a statistical classification based on an application of neural networks by Multilayer Perceptron (MLP) to classify

Partial Discharge (PD) patterns that is a one way simulation to analyze and classify PD patterns.

MATERIALS AND METHOD

1. Partial Discharge experiments and pattern analysis in high voltage apparatus

From the experiment to simulate the partial discharge pattern, it can actually occur in high voltage equipment according to the IEC 60270 Standard (IEC, 2000) as the partial discharge test and measurement. There are four types of partial discharge patterns that can occur in high-voltage devices: high voltage side in air, corona at low voltage side in air, surface in air, and internal discharge. The PD simulation was performed in a chamber with a flat plate electrode of 12 cm in diameter. The model had the following defect patterns: simulations and experimental as for the results from Vicetjindavat (2001).

1. Simulation of the corona discharge in the air as the discharge occurs in the pointed region, it is the region of high electric field stress. By bringing a copper wire of diameter 0.1 cm, length 1.5 cm, it was attached to the high-voltage electrode and the low voltage side with a distance between the electrodes 10 cm as shown in Figure 1. When the voltage is applied, the electric field stresses at the ends of the windings resulting in the corona being generated.

2. Simulation of internal discharge within a solid insulator is done by simulating small air cavities within the 13×13×2.5 cm. Acrylic sheet will cause a voltage drop across different parts of the insulator. The simulation is done in the oil chamber to prevent flashover across the solid insulation. If the pressure drops across the gas cavity is higher than the pressure that the gas cavity can withstand, it may cause break-down or discharge only in the gas cavity. There are different simulation models as shown in Figure 2.

a) Corona discharge at high voltage side in air b) Corona discharge at low voltage side in air

Figure 1 Corona discharge voltage side in air simulation.

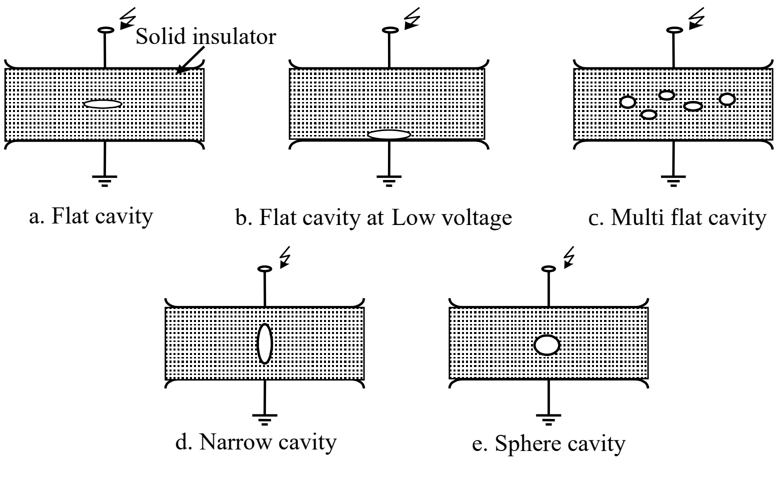

Figure 2 Corona discharge of internal discharge simulation.

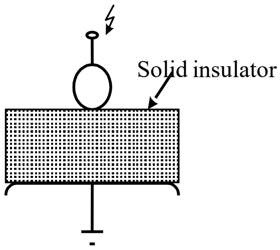

Figure 3 Corona discharge of surface discharge simulation.

3. The simulation of surface discharge is made by using an acrylic sheet between a 5 cm. diameter circular electrode and a 12 cm. diameter flat sheet electrode. The junctions of two types of insulators with different percentage values are air and acrylic sheets as shown in Figure 3.

The experiment simulating a partial discharge pattern can actually occur in high-voltage equipment according to the IEC 60270 Standard (IEC, 2000). There are four categories of partial discharge patterns that can occur in high-voltage devices : featuring four categories in corona: high voltage side in air, corona at low voltage side in air, surface in air, and internal discharge. The PD simulation was performed in a chamber with a flat plate electrode measuring 12 cm. in diameter. The experimental results from (Vicetjin davat, 2001).

The partial discharge model simulations,7 experiments were conducted (Vicetjindavat, 2001), of which 20 were simulated corona at high voltage side in air. ; Corona at HV, (20 trials later. This is an experiment to simulate the corona at low voltage side in air; Corona at L.V.) 19 subsequent trials. These experiments simulated internal discharge patterns and 20 experiments were surface in air simulated experiments. Based on the data, 79 experiments were randomized to 80 experiments for convenience. Following the matrix calculation, the partial discharge pattern data obtained from each partial discharge (PD) monitor were analyzed. There are 9 independent variables from fingerprint analysis which mainly are skewness, kurtosis, asymmetry and cross correlation followingPhi-q-n. PD patterns were used for classification consists of statistical attribute calculation values. This is calculated from the average PD size distribution based on the voltage phase angle (Hqn(ϕ)) and the number of PD repeat distributions based on the voltage phaseangle (ϕ)).The relationship between the magnitude of the PD (q), the phase angle of the test voltage(ϕ) and the number of PD repetitions (n) is shown in Figure 4-7 and Table 1-8, respectively. The PD detector calculates the statistical properties of Skewness (Sk) and Kurtosis (Ku) of $H_{qn}(\phi)$ and $H_n(\phi)$ which gives a total of 9 variables in the matrix X: Sk^+ of $H_{qn}(\phi)$, Sk^- of $H_{qn}(\phi)$, Ku^+. of $H_{qn}(\phi)$,Ku^- of $H_{qn}(\phi)$, Sk^+ of $H_n(\phi)$, Sk^- of $H_n(\phi)$, Ku^+ of $H_n(\phi)$,Ku^- of $H_n(\phi)$, and the apparent charge (Q) (Vicetjindavat, 2001).

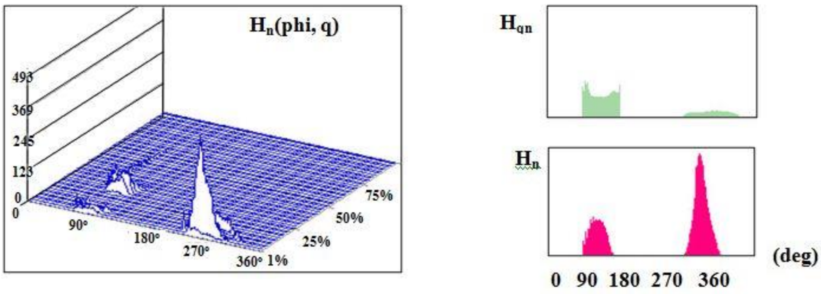

Figure 4 Examples of simulation results of corona at high voltage side in air patterns.

Table 1 Examples statistical value of corona at high voltage side in air patterns.

	Statistical Operations						
	Sk^+	**Sk^-**	**Ku^+**	**Ku^-**	**Q**	**CC**	**mcc**
H_{qn}	1.034	1.014	-1.915	-1.964	0.238	0.785	0.187
H_n	1.100	1.092	-1.739	-1.748			

Table 2 Example of data collection of corona at high voltage side in air patterns simulation results. (Vicetjindavat, 2001)

No.	PD Patterns	Sk^+ of $H_{qn}(\emptyset)$	Sk^- of $H_{qn}(\emptyset)$	Ku^+ of $H_{qn}(\emptyset)$	Ku^- of $H_{qn}(\emptyset)$	Sk^+ of $H_n(\emptyset)$	Sk^- of $H_n(\emptyset)$	Ku^+ of $H_n(\emptyset)$	Ku^- of $H_n(\emptyset)$	Q
1	Corona at High Voltage side in air	1.188	1.077	-1.507	-1.983	1.220	1.093	-1.393	-1.696	0.359
2		1.312	1.016	-1.174	-1.959	1.334	1.131	-1.053	-1.630	0.424
3		1.482	1.025	-0.616	-1.935	1.339	1.126	-1.073	-1.659	0.425
4		1.270	1.022	-1.276	-1.944	1.152	1.106	-1.592	-1.699	0.815
5		1.166	1.008	-1.568	-1.979	1.191	1.167	-1.482	-1.495	0.384
6		1.277	1.028	-1.246	-1.929	1.144	1.112	-1.605	-1.680	0.778
7		1.016	1.024	-1.958	-1.938	1.030	1.038	-1.923	-1.885	0.227
8		1.100	1.030	-1.741	-1.919	1.179	1.102	-1.528	-1.727	0.382
9		1.025	1.007	-1.936	-1.982	1.063	0.965	-1.837	-2.039	0.321
10		1.028	1.006	-1.929	-1.983	1.062	0.951	-1.839	-0.720	0.336
11		1.034	1.005	-1.913	-1.988	1.091	0.981	-1.763	-1.997	0.331
12		1.031	1.018	-1.922	-1.953	1.077	0.947	-1.800	-2.081	0.175
13		1.034	1.015	-1.914	-1.962	1.089	1.012	-1.769	-1.901	0.226
14		1.025	1.021	-1.936	-1.946	1.072	0.939	-1.813	-2.068	0.231
15		1.034	1.014	-1.915	-1.964	1.100	1.092	-1.739	-1.748	0.238
16		1.020	1.020	-1.950	-1.947	1.053	0.919	-1.862	-2.126	0.239
17		1.026	1.010	-1.935	-1.972	1.085	1.036	-1.779	-1.856	0.242
18		1.010	1.020	-1.974	-1.947	1.022	0.942	-1.942	-2.082	0.236
19		1.061	1.021	-1.841	-1.946	1.138	0.085	-1.638	-2.331	0.258
20		1.025	1.012	-1.936	-1.970	1.086	1.080	-1.776	-1.768	0.248

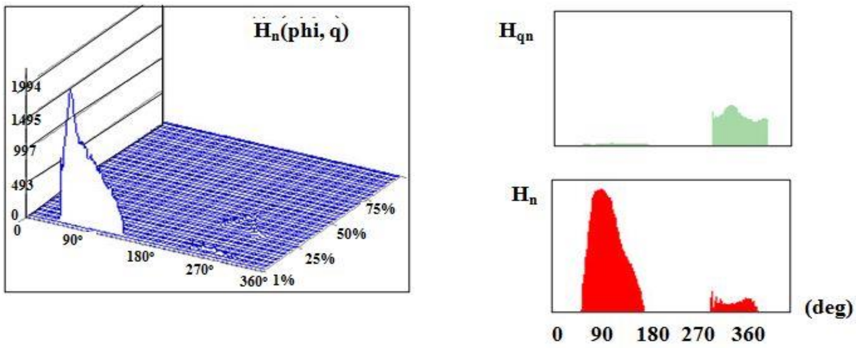

Figure 5 Examples of simulation results of corona at low voltage side in air patterns.

Table 3 Examples statistical value of corona at low voltage side in air patterns.

	Statistical Operations						
	Sk^+	**Sk^-**	**Ku^+**	**Ku^-**	**Q**	**CC**	**mcc**
H_{qn}	1.007	1.012	-1.981	-1.969	7.104	0.832	5.909
H_n	1.010	-0.340	-1.974	-2.884			

Table 4 Data collection of corona at low voltage side in air patterns simulation results. (Vicetjindavat, 2001)

No.	PD Patterns	Sk^+ of $H_{qn}(\emptyset)$	Sk^- of $H_{qn}(\emptyset)$	Ku^+ of $H_{qn}(\emptyset)$	Ku^- of $H_{qn}(\emptyset)$	Sk^+ of $H_n(\emptyset)$	Sk^- of $H_n(\emptyset)$	Ku^+ of $H_n(\emptyset)$	Ku^- of $H_n(\emptyset)$	Q
21		1.014	1.085	-1.960	-1.780	1.056	-0.410	-1.850	-2.830	6.975
22		1.015	1.017	-1.960	-1.960	1.021	-0.440	-1.940	-2.810	5.225
23		1.010	1.019	-1.980	-1.950	1.015	-0.320	-1.960	-2.900	7.591
24		1.015	1.017	-1.960	-1.960	1.021	-0.440	-1.940	-2.810	5.225
25		1.009	1.015	-1.980	-1.960	1.066	-0.300	-1.980	-2.910	8.540
26		1.007	1.012	-1.980	-1.970	1.010	-0.340	-1.970	-2.880	7.104
27		1.013	1.020	-1.970	-1.950	1.071	-0.680	-1.810	-2.520	3.717
28		1.007	1.012	-1.980	-1.970	1.010	-0.340	-1.970	-2.880	7.104
29		1.015	1.015	-1.960	-1.960	1.045	-0.600	-1.880	-2.640	4.000
30	Corona at low Voltage side in air	1.012	1.017	-1.970	-1.960	1.064	-0.640	-1.830	-2.580	3.954
31		1.005	1.014	-1.970	-1.960	1.030	-0.520	-1.920	-2.730	5.200
32		1.011	1.008	-1.970	-1.980	1.048	-0.620	-1.870	-2.610	3.700
33		1.008	1.015	-1.980	-1.960	1.053	-0.660	-1.860	-2.560	3.751
34		1.008	1.011	-1.980	-1.970	1.050	-0.630	-1.870	-2.600	3.639
35		1.016	1.065	-1.960	-1.830	1.074	-0.670	-1.800	-2.550	4.233
36		1.006	1.031	-1.990	-1.920	1.059	-0.660	-1.840	-2.560	4.110
37		1.010	1.012	-1.970	-1.970	1.025	-0.530	-1.930	-2.720	4.614
38		1.007	1.012	-1.980	-1.970	1.072	-0.680	-1.810	-2.530	3.658
39		1.010	1.010	-1.970	-1.970	1.048	-0.610	-1.870	-2.620	4.065
40		1.014	1.032	-1.960	-1.920	1.040	-0.570	-1.890	-2.670	4.341

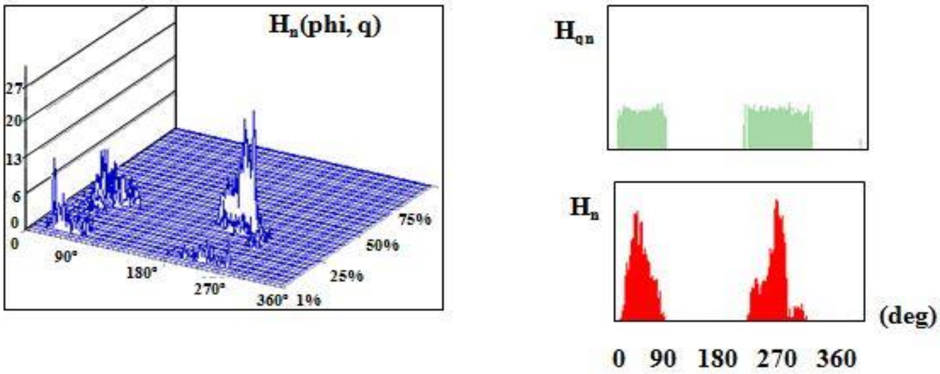

Figure 6 Examples of simulation results of corona internal discharge patterns.

Table 5 Examples statistical value of corona internal discharge patterns.

	Statistical Operations						
	Sk^+	**Sk^-**	**Ku^+**	**Ku^-**	**Q**	**CC**	**mcc**
H_{qn}	1.044	1.168	-1.889	-1.438	0.985	0.786	0.774
H_n	1.006	-0.222	-1.984	-2.398			

Table 6 Data collection of corona internal discharge patterns simulation results. (Vicetjindavat, 2001)

No.	**PD Patterns**	**Sk^+ of $H_{qn}(\emptyset)$**	**Sk^- of $H_{qn}(\emptyset)$**	**Ku^+ of $H_{qn}(\emptyset)$**	**Ku^- of $H_{qn}(\emptyset)$**	**Sk^+ of $H_n(\emptyset)$**	**Sk^- of $H_n(\emptyset)$**	**Ku^+ of $H_n(\emptyset)$**	**Ku^- of $H_n(\emptyset)$**	**Q**
41		1.124	1.172	-1.700	-1.540	1.226	-0.760	-1.430	-2.340	1.132
42		1.178	1.142	-1.480	-1.620	1.145	-0.730	-1.640	-2.320	1.171
43		1.504	1.479	0.103	-0.020	1.345	-0.280	0.708	-2.370	1.015
44		1.504	1.479	0.103	-0.020	1.345	-0.280	-0.710	-2.370	1.015
45		1.206	1.200	-1.470	-1.490	1.307	-0.220	-0.960	-2.380	1.038
46		1.491	1.202	-0.030	-1.490	1.524	-0.210	0.305	-2.310	1.063
47		1.193	1.178	-1.510	-1.550	1.240	-0.110	-1.360	-2.360	1.036
48		1.192	1.482	-1.510	-0.170	1.226	-0.250	-1.430	-2.370	1.059
49		1.186	1.165	-1.530	-1.590	1.189	-0.430	-1.520	-2.380	1.037
50	Internal Discharge	1.170	1.154	-1.570	-1.610	1.168	-0.680	-1.560	-2.330	1.149
51		1.147	1.175	-1.630	-1.540	1.180	-0.710	-1.520	-2.320	1.191
52		1.115	1.106	-1.710	-1.730	1.132	-0.760	-1.640	-2.330	1.250
53		1.178	1.142	-1.480	-1.620	1.145	-0.730	-1.640	-2.320	1.172
54		1.073	1.103	-1.830	-1.730	1.077	-0.610	-1.820	-2.340	1.057
55		1.142	1.100	-1.630	-1.750	1.125	-0.50	-1.640	-2.370	1.073
56		1.115	1.153	-1.710	-1.600	1.110	-0.370	-1.730	-2.390	1.107
57		1.141	1.152	-1.630	-1.600	1.113	-0.430	-1.710	-2.390	1.136
58		1.133	1.153	-1.660	-1.580	1.124	-0.630	-1.680	-2.340	1.125
59		1.104	1.106	-1.730	-1.710	1.073	-0.690	-1.810	-2.320	1.304
60		1.178	1.142	-1.480	-1.620	1.145	-0.730	-1.640	-2.320	1.172

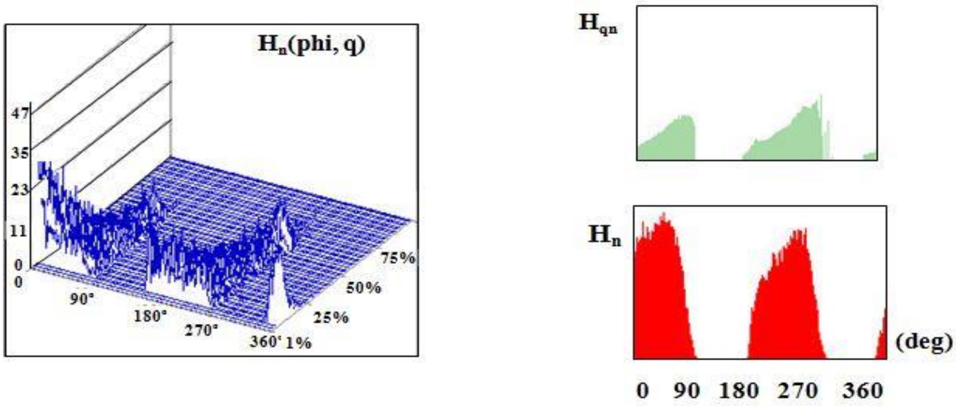

Figure 7 Examples of simulation results of corona surface in air patterns.

Table 7 Examples statistical value of corona surface in air patterns.

	Statistical Operations						
	Sk^+	**Sk^-**	**Ku^+**	**Ku^-**	**Q**	**CC**	**mcc**
H_{qn}	1.504	1.330	-0.184	-0.844	1.139	0.867	0.988
H_n	1.985	-0.453	1.781	-2.252			

Table 8 Data collection of corona surface in air patterns simulation results. (Vicetjindavat, 2001)

No.	**PD Patterns**	**Sk^+ of $H_{qn}(\emptyset)$**	**Sk^- of $H_{qn}(\emptyset)$**	**Ku^+ of $H_{qn}(\emptyset)$**	**Ku^- of $H_{qn}(\emptyset)$**	**Sk^+ of $H_n(\emptyset)$**	**Sk^- of $Hn(\emptyset)$**	**Ku^+ of $H_n(\emptyset)$**	**Ku^- of $H_n(\emptyset)$**	**Q**
61		1.442	1.464	-0.450	-0.270	1.986	-0.680	1.967	-2.510	1.462
62		1.461	1.302	-0.230	-1.000	1.939	1.906	1.607	1.430	0.805
63		1.453	1.170	-0.300	-1.490	1.942	1.899	1.667	1.569	0.786
64		1.529	1.230	-0.030	-1.300	1.747	1.841	0.470	1.268	0.861
65		1.465	1.241	-0.270	-1.240	1.925	1.797	1.466	1.178	0.881
66		1.463	1.188	-0.280	-1.430	1.956	1.332	1.613	-0.070	0.901
67		1.446	1.189	-0.390	-1.410	1.995	-0.100	1.813	-2.050	1.093
68		1.529	1.278	-0.050	-1.130	1.714	1.867	2.900	1.211	0.873
69		1.504	1.330	-0.180	-0.840	1.985	-0.450	1.781	-2.250	1.139
70		1.457	1.379	-0.400	-0.670	1.967	-0.350	1.669	-2.210	1.072
71	Surface in air	1.486	1.423	-0.250	-0.490	1.955	-0.120	1.597	-2.070	1.009
72		1.501	1.383	-0.180	-0.640	1.968	-0.410	1.754	-2.250	1.134
73		1.467	1.450	-0.360	-0.360	1.943	-0.570	1.620	-2.340	1.176
74		1.511	1.479	-0.180	-0.220	1.977	-0.690	1.923	-2.390	1.355
75		1.481	1.428	-0.410	-0.500	1.919	-0.610	1.365	-2.390	1.081
76		1.516	1.471	-0.160	-0.250	1.976	-0.690	1.919	-2.390	1.364
77		1.493	1.471	-0.260	-0.280	1.918	-0.460	1.451	-2.300	1.163
78		1.496	1.450	-0.270	-0.390	1.954	-0.590	1.702	-2.350	1.206
79		1.459	1.302	-0.390	-1.000	1.952	-0.630	1.647	-2.360	1.225
80		1.486	1.454	-0.340	-0.410	1.919	-0.540	1.408	-2.350	1.078

The results of analysis of variance (ANOVA) in testing the mean of each variable were different between groups or not. Analysis of Variance (ANOVA) is an analysis to test the mean difference of more than 2 groups (3 or more groups). That is to compare 2 parts, namely, between the group and within the group, in order to find the variables related to each other. Selecting input variables into the equation. First of all, it is necessary to consider which independent variables are likely to be associated with the dependent variable Y, both positive and negative, and the relationship between the group variables of each independent variable. In this study, the F test and Wilks'Lambda statistical tests were used to help exclude correlated variables as shown in Table 9.

Table 9 Results of Analysis of Variance (ANOVA) in the mean test of each variable whether they differed between groups or not.

Variable	Wilks'Lambda	F	df1	df2	Sig.
Sk^+ of $H_{qn}(\emptyset)$	0.214	92.920	3	76	.000
$Sk^-$of $H_{qn}(\emptyset)$	0.255	74.021	3	76	.000
$Ku^+$of $H_{qn}(\emptyset)$	0.231	84.488	3	76	.000
$Ku^-$of $H_{qn}(\emptyset)$	0.343	48.527	3	76	.000
$Sk^+$of $H_n(\emptyset)$	0.047	514.879	3	76	.000
$Sk^-$of $H_n(\emptyset)$	0.442	32.044	3	76	.000
$Ku^+$of $H_n(\emptyset)$	0.076	308.584	3	76	.000
$Ku^-$of $H_n(\emptyset)$	0.696	11.046	3	76	.000
Q	0.148	146.162	3	76	.000
cc	0.962	1.001	3	76	.397

Based on the test's Sig value, it was found to be all 0 except for the variable cc which was 0.397, and it was greater than the specified significance level of 0.01. It can be seen that

- The mean of all variables except cc variable differs between groups.

- The mean of cc variables did not differ between groups which was concluded from at least one pair of tests;

- Test Sig = 0.397, H_0 cannot be rejected. Therefore, cc should not be a variable used to classify groups. The variable mcc is the result of multiplying between variable cc and variable Q, thus eliminating. Therefore, the remaining 9 variables are taken into account.

2. PD Classification method and model simulation

In this paper will use statistical modeling methods. The data used in the simulation consisted of matrix X and matrix Y, where matrix X is the input variable measured by the partial discharge detector, consisting of $H_{qn}(\phi)$ (average PD size distribution. according to the phase angle of the voltage), $H_n(\phi)$ (the number of PD repetitions distribution according to the voltage phase angle), Q (appearance charge), for which the PD detector calculates the statistical property of Skewness (Sk) and Kurtosis (Ku) of $H_{qn}(\phi)$ and $H_n(\phi)$ gives a total of 9 variables in the matrix X: Sk^+ of $H_{qn}(\phi)$, Sk^- of $H_{qn}(\phi)$, Ku^+. of $H_{qn}(\phi)$,Ku^- of $H_{qn}(\phi)$, Sk^+ of $H_n(\phi)$, Sk^- of $H_n(\phi)$, Ku^+ of $H_n(\phi)$,Ku^- of $H_n(\phi)$, and the apparent charge (Q), whose the matrix has a size of 80 × 9. The Y matrix is a dummy variable used to predict each type of partial discharge, and the matrix has a size of 80 × 1. Based on the data, 79 trials were randomized to 80 trials for ease of calculation matrix.

1. From the X matrix, the data were divided into 4 groups: rows 1 to 20 were variable data values for Corona at High Voltage side in air (Corona at H.V.), rows 21 to 40 were data values of Corona at Low Voltage side in air (Corona at LV), rows 41 to 60 were internal discharge, rows 61 to 80 were Surface in air and The Y matrix is a hypothetical variable to classify the PD, with the code for division 1 to 20, designated as [1] and given as Corona. at HV Rows 21 to 40 are designated as [2] and given as Corona at LV. Rows 41 to 60 are designated as [3] and given as Internal Discharge. Rows 61 to 80 designated as [4] and given as Surface. Discharge has a structure as in Eq. (1).

$$X = \begin{bmatrix} [Corona\ at\ H.V.]_{20x9} \\ [Corona\ at\ L.V.]_{20\times9} \\ [Internal\ Discharge]_{20\times9} \\ [Surface\ Discharge]_{20\times9} \end{bmatrix}_{80\times9} \quad Y = \begin{bmatrix} [1]_{20\times1} \\ [2]_{20\times1} \\ [3]_{20\times1} \\ [4]_{20\times1} \end{bmatrix}_{80\times1} \tag{1}$$

2. Scaled the input matrix X to unify the data and control the variance of the scaled data because in the modeling, the importance of each variable in the X matrix is equal to all variables. is to make the variances of each variable in the X matrix or input matrix equal to 1.

3. Divide the scaled matrix data into two groups: the learning data group (train) to create the model and the test data group (test) to experiment with the model. The dividing method is divided into Venetial Blinds (VB) and the data is rearranged in the XVB matrix and the YVB matrix as shown in Eq. (2).

$$XVB = \begin{bmatrix} [Xtrain] \\ [Xtest] \end{bmatrix}_{80\times9} \quad YVB = \begin{bmatrix} [Ytrain] \\ [Ytest] \end{bmatrix}_{80\times1} \tag{2}$$

4. The model was simulated by using multilayer perceptron Analysis. It was found that there were 9 variable input layers, 1 hidden layer and an output layer as shown in the Figure 8 - Figure 9.

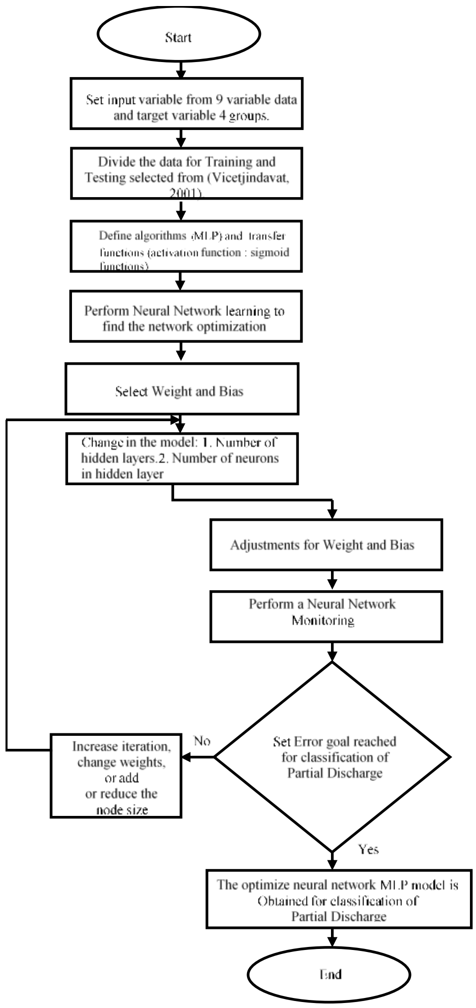

Figure 8 Flow chart of multilayer perceptron model.

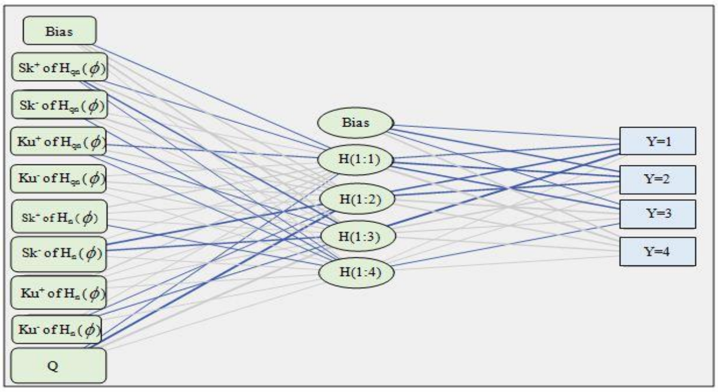

Figure 9 Network of simulation results of multilayer perceptron model.

RESULTS AND DISCUSSION

Simulation results

In this paper, the researchers examined how to classify the type of PD by a multilayer perceptron. The architecture is simple and easy. It is used for the pattern classification system and it can also reduce the time to compute results for faster and more flexible than statistical methods (Chatpattananan, 2006; Chatpattananan *et al*., 2006a). It can also calculate and get accurate results just like the method used Regression Estimation (Ludpa *et al*., 2008; Pattanadech *et al*., 2015a). A Multilayer Perceptron with a hidden layers can design arbitrary classification,and the approximation is related to the number of hidden nodes. The neuron number of its input is determined by the number of statistical features, skewness, kurtosisand. The neuron number of both hidden layers is 1. The neuron number of output layer is determined by the number of patterns to be identified, comprised 4 groups : corona at high voltage side in air (corona at H.V.), corona at low voltage side in air (corona at LV), internal discharge and surface in air, respectively. To demonstrate the classification ability, 80 sets of field test PD patterns are used to test the proposed PD classification system. The neural network based PD classification system randomly chooses 80 instances from the field test data as the training data set, and the rest of the instances of the field test data are the testing data set. Table 10 - 14 shows the classified results of the proposed system with different input patterns. The recognition rates of the proposed system are quite high with 100%. It is obvious that the neural network based PD classification system has strong generalized capability. It is obvious that the neural network based PD classification system has strong generalized capability to evaluate the fault tolerance ability.

Table 10 Model Summary

Training	Cross Entropy Error	0.271
	Percent Incorrect Classification	0.00%
	Stopping Rule Used	1 consecutive step (s) with no decrease in error[a]
	Train Time	0:00:00.022
Testing	Cross Entropy Error	0.494
	Percent Incorrect Classification	0.00%

Table 11 Parameter Classification

Parameter		Classification							
		Hidden Layer 1				Output Layer			
		H(1:1)	H(1:2)	H(1:3)	H(1:4)	[Y=1]	[Y=2]	[Y=3]	[Y=4]
Input Layer	(Bias)	0.492	0.916	0.980	0.009				
	Sk^{+} of $H_{qn}(\phi)$	0.204	1.119	0.716	0.060				
	Sk^{-} of $H_{qn}(\phi)$	0.333	1.832	0.327	0.428				
	Ku^{+} of $H_{qn}(\phi)$	0.935	0.983	0.078	0.108				
	Ku^{-} of $H_{qn}(\phi)$	0.093	1.010	0.768	0.276				
	Sk^{+} of $H_{n}(\phi)$	1.084	0.171	0.655	0.173				
	Sk^{-} of $H_{n}(\phi)$	0.456	-2.357	-1.501	0.159				
	Ku^{+} of $H_{n}(\phi)$	0.803	0.224	0.753	0.709				
	Ku^{-} of $H_{n}(\phi)$	0.455	-0.102	0.705	0.024				
	Q	0.667	-1.300	2.904	0.589				
Hidden Layer 1	(Bias)					0.264	-1.109	0.086	1.008
	H(1:1)					0.951	-2.418	-1.361	5.143
	H(1:2)					-1.803	-1.892	3.266	1.149
	H(1:3)					-3.703	1.775	0.867	1.109
	H(1:4)					0.204	580.000	0.631	0.344

Table 12 Classification Results

Sample	Observed	Classification				
		1	2	3	4	Percent Correct
Training	1	16	0	0	0	100.0%
	2	0	16	0	0	100.0%
	3	0	0	10	0	100.0%
	4	0	0	0	14	100.0%
	Overall Percent	28.60%	28.60%	17.90 %	25.00 %	100.0%
Testing	1	4	0	0	0	100.0%
	2	0	4	0	0	100.0%
	3	0	0	10	0	100.0%
	4	0	0	0	6	100.0%
	Overall Percent	16.70%	16.70%	41.70 %	25.00 %	100.0%

Table 13 Examples Training Value of Classification Results

Training									
Input (X)									Target (Y)
Sk^+ of $H_{qn}(\phi)$	Sk^- of $H_{qn}(\phi)$	Ku^+ of $H_{qn}(\phi)$	Ku^- of $H_{qn}(\phi)$	Sk^+ of $H_n(\phi)$	Sk^- of $H_n(\phi)$	Ku^+ of $H_n(\phi)$	Ku^- of $H_n(\phi)$	Q	
1.188	1.077	-1.507	-1.983	1.220	1.093	-1.393	-1.696	0.359	1
1.312	1.016	-1.174	-1.959	1.334	1.131	-1.053	-1.630	0.424	1
1.482	1.025	-0.616	-1.935	1.339	1.126	-1.073	-1.659	0.425	1
1.270	1.022	-1.276	-1.944	1.152	1.106	-1.592	-1.699	0.815	1
1.014	1.085	-1.960	-1.780	1.056	-0.410	-1.850	-2.830	6.975	2
1.015	1.017	-1.960	-1.960	1.021	-0.440	-1.940	-2.810	5.225	2
1.010	1.019	-1.980	-1.950	1.015	-0.320	-1.960	-2.900	7.591	2
1.015	1.017	-1.960	-1.960	1.021	-0.440	-1.940	-2.810	5.225	2
1.124	1.172	-1.700	-1.540	1.226	-0.760	-1.430	-2.340	1.132	3
1.178	1.142	-1.480	-1.620	1.145	-0.730	-1.640	-2.320	1.171	3
1.504	1.479	0.103	-0.020	1.345	-0.280	0.708	-2.370	1.015	3
1.504	1.479	0.103	-0.020	1.345	-0.280	-0.710	-2.370	1.015	3
1.442	1.464	-0.450	-0.270	1.986	-0.680	1.967	-2.510	1.462	4
1.461	1.302	-0.230	-1.000	1.939	1.906	1.607	1.430	0.805	4
1.453	1.170	-0.300	-1.490	1.942	1.899	1.667	1.569	0.786	4
1.529	1.230	-0.030	-1.300	1.747	1.841	0.470	1.268	0.861	4

Table 14 Examples Testing Value of Classification Results

Testing									Target (Y)	MLP Classification Result	Accuracy (%)
Input (X)											
Sk^+ of $H_{qn}(\phi)$	Sk^- of $H_{qn}(\phi)$	Ku^+ of $H_{qn}(\phi)$	Ku^- of $H_{qn}(\phi)$	Sk^+ of $H_n(\phi)$	Sk^- of $H_n(\phi)$	Ku^+ of $H_n(\phi)$	Ku^- of $H_n(\phi)$	Q			
1.026	1.010	-1.935	-1.972	1.085	1.036	-1.779	-1.856	0.242	1	1	100
1.010	1.020	-1.974	-1.947	1.022	0.942	-1.942	-2.082	0.236	1	1	100
1.061	1.021	-1.841	-1.946	1.138	0.085	-1.638	-2.331	0.258	1	1	100
1.025	1.012	-1.936	-1.970	1.086	1.080	-1.776	-1.768	0.248	1	1	100
1.010	1.012	-1.970	-1.970	1.025	-0.530	-1.930	-2.720	4.614	2	2	100
1.007	1.012	-1.980	-1.970	1.072	-0.680	-1.810	-2.530	3.658	2	2	100
1.010	1.010	-1.970	-1.970	1.048	-0.610	-1.870	-2.620	4.065	2	2	100
1.014	1.032	-1.960	-1.920	1.040	-0.570	-1.890	-2.670	4.341	2	2	100
1.147	1.175	-1.630	-1.540	1.180	-0.710	-1.520	-2.320	1.191	3	3	100
1.115	1.106	-1.710	-1.730	1.132	-0.760	-1.640	-2.330	1.25	3	3	100
1.178	1.142	-1.480	-1.620	1.145	-0.730	-1.640	-2.320	1.172	3	3	100
1.073	1.103	-1.830	-1.730	1.077	-0.610	-1.820	-2.340	1.057	3	3	100
1.481	1.428	-0.410	-0.500	1.919	-0.610	1.365	-2.390	1.081	4	4	100
1.516	1.471	-0.160	-0.250	1.976	-0.690	1.919	-2.390	1.364	4	4	100
1.493	1.471	-0.260	-0.280	1.918	-0.460	1.451	-2.300	1.163	4	4	100
1.496	1.450	-0.270	-0.390	1.954	-0.590	1.702	-2.350	1.206	4	4	100

CONCLUSION

The proposed method to analyze PD patterns and classify the type of discharge is an important tool for the diagnosis of a high voltage insulation system. To improve the performance, are statistically analyzed for the proposed multilayer perceptron classifier. These statistical features are then applied to a neural network that performs the classification. The recognition rates of the proposed system are quite high at 100%. The present experimental results indicate that this approach is able to implement an efficient classification with a very high recognition rate. The proposed method can use to analyze and classify partial discharge patterns and it can be developed to test the partial discharge of high voltage equipment.

ACKNOWLEDGEMENTS

The authors would like to give special acknowledgement to the School of Engineering, King Mongkut's Institute of Technology Ladkrabang for providing the facility in this research.

REFERENCES

Chatpattananan, V. 2006. Linear Discriminant Analysis for Partial Discharge Classification on High Voltage Equipment, pp. 627- 630. *In* **Conference on Electrical Insulation and Dielectric Phenomena, (CEIDP).** IEEE, Kansas City, MO, USA.

Chatpattananan, V., Pattanadech, N. and Vicetjindavat, K. 2006a. PCA-LDA for Partial Discharge Classification on High voltage Equipment, pp. 479-481. *In* **Proceedings of 8th International Conference on Properties and applications of Dielectric Materials.** IEEE, Bali, Indonesia.

Chatpattananan, V., Pattanadech, N. and Vicetjindavat, K. 2006b. Quest Tree Model for Partial Discharge Classification on High voltage Equipment, pp.476-478. *In* **Proceedings of 8th International Conference on Properties and applications of Dielectric Materials.** IEEE, Bali, Indonesia.

Chatpattananan, V., Pattanadech, N. and Yutthagowith, P. 2006c. Partial Discharge Classification on High Voltage Equipment with K-Means, pp. 191-194. *In* **Proceedings of 8th International Conference on Properties and applications of Dielectric Materials.** IEEE, Bali, Indonesia.

Cho, K.B. and Oh, J.Y. 1997. An Overview of Application of Artificial Neural Network to Partial Discharge Pattern Classification, pp.326-330. *In* **Proceedings of 5th International Conference on Properties and Applications of Dielectric Materials.** IEEE, Seoul, Korea (South).

Gopal, S., Karthikeyan, B. and Kavitha, D. 2004. Partial discharge pattern classification using fuzzy expert system, pp. 653-656. *In* **Proceedings of the 2004 IEEE International Conference on Solid Dielectrics.** IEEE, Toulouse, France.

Gulski, E. and Krivda, A. 1993. Neural Networks as a Tool for Recognition of Partial Discharges. **IEEE Transactions on Electrical Insulation** 28(6): 984-1001.

IEC. 2000. **IEC 60270 International Standard High-voltage test techniques - Partial discharge measurements.** 3rd ed. IEC, Geneva, Switzerland.

Ludpa, S., Pattanadech, N., Leelajindakrairerk, M. and Yutthagowith, P. 2008. Pattern Classification of Partial Discharge in High Voltage Equipment by Regression Analysis, pp. 921-924. *In* **5th International Conference on Electrical Engineering / Electronics, Computer,Telecommunications and Information Technology 2.** IEEE, Krabi, Thailand.

Pattanadech, N. and Nimsanong, P. 2014. Partial discharge classification using principal component analysis combined with self-organizing map, pp. 1-5. *In* **TENCON 2014 - 2014 IEEE**

Region 10 Conference. IEEE, Bangkok, Thailand.

Pattanadech, N., Nimsanong, P., Potivejkul, S., Yuthagowith, P. and Polmai, S. 2015a. Partial discharge classification using probabilistic neural network model, pp. 1176-1180. *In* **18th International Conference on Electrical Machines and Systems (ICEMS).** IEEE, Pattaya, Thailand.

Pattanadech, N., Nimsanong, P., Potivejkul, S., Yuthagowith, P. and Polmai, S. 2015b. Generalized regression networks for partial discharge classification, pp. 1165-1169. *In* **18th International Conference on Electrical Machines and Systems (ICEMS).** IEEE, Pattaya, Thailand.

Tomsovic, K., Tapper, M. and Ingvarsson, T.T. 1993. A Fuzzy Information Approach to Integrating Different Transformer Diagnostic methods. **IEEE Transactions on Power Delivery** 8: 1638-1643.

Vicetjindavat, K. 2001. Pattern Recognition of Partial Discharge in High Voltage Equipment. Master Thesis of Engineering, Department of Electrical Engineering, Chulalongkorn University.

Zhang, H., Lee, W.J., Kwan, C., Ren, Z., Chen, H. and Sheeley, J. 2005. Artificial Neural Network Based On-Line Partial Discharge Monitoring System for Motors, pp. 125-132. *In* **IEEE Systems Technical Conference on Industrial and Commercial Power 2005.** IEEE, Saragota Springs, NY, USA.